5-2016

Graphene and Carbon Nanotube PLA Composite Feedstock Development for Fused Deposition Modeling

Austin Plymill
University of Tennessee, Knoxville, pjr293@vols.utk.edu

Robert Minneci
University of Tennessee, Knoxville, rminneci@vols.utk.edu

Duncan Alexander Greeley
University of Tennessee - Knoxville

Jack Gritton
University of Tennessee, Knoxville, jgritton@vols.utk.edu

Graphene and Carbon Nanotube PLA Composite Feedstock Development for Fused Deposition Modeling

Duncan Greeley, Jack Gritton, Robert Minneci, Austin Plymill
MSE 489 - Senior Design

Faculty Advisor: Dr. Gajanan Bhat
Industry Partner: NatureWorksLLC
Funding Provided by the University of Tennessee, Knoxville

Abstract

Additive manufacturing shows significant potential for replacement of traditionally manufactured parts, part repair, and prototype development due to complexity of allowable part geometry and low raw material usage, however mechanical properties of parts processed through additive typically suffer in comparison. To address this decrease in properties, the goal of this study will be to develop an improved and sustainable feedstock material for fused deposition modeling through reinforcement of polylactic acid with graphene and multiwalled carbon nanotubes. Composites with loadings of 0.5, 0.2, and 0.1 wt% of each reinforcement were extruded to form filament feedstock for fused deposition modeling, and tensile and impact specimens were printed using a Lulzbot Mini according to ASTM D638 and D256. Mechanical properties were evaluated through tensile and impact testing, while fracture surfaces were analyzed using a scanning electron microscope. The thermal properties of the feedstock material and post-printed material were analyzed with differential scanning calorimetry. Reinforcements led to a moderate increase in mechanical properties with the 0.2 wt% loading of graphene showing a 47% increase in tensile strength, a 17% increase in modulus, and 12% increase in energy absorbed upon fracture. The 0.1 wt% loading of MWCNT had respective increases of 41%, 16%, and 9%, with all reinforcement loadings leading to no statistically significant change in the thermal properties or fracture behavior.

1 Introduction

Additive manufacturing (AM) has been increasingly implemented over the past several years as an efficient means to prototype and produce components with a high degree of shape complexity. When compared to traditional subtractive processes, AM allows for a reduction in raw material use which leads to significant cost savings through a lower buy-to-fly ratio (weight ratio between raw material and final part). However as AM is a fairly new process, parts manufactured in this method tend to have downsides compared to parts manufactured through traditional methods, namely reduced mechanical properties and property anisotropy due to the bonding strength between layers and porosity in the final structure [1]. For the purpose of this study we will be investigating additive processing of polymeric materials as opposed to metals, as they offer significant flexibility in feedstock modification through additives or reinforcements. One of the most promising methods of improving the mechanical properties of polymeric parts involves reinforcement of the polymer resin with a strong, lightweight material dispersed throughout the matrix. For instance, carbon fiber is often used to increase the strength and stiffness of several types of polymers. The improvements of these properties in the final product typically follows a simple rule of mixtures for uniaxially oriented fibers such as in the case for the tensile modulus:

$$E = (1-V_f)E_m + V_fE_f \quad (1)$$

where E is the longitudinal modulus, V_f is the volume fraction of the fiber, E_m is the modulus of the matrix, and E_f is the modulus of the fiber [2].

As fused deposition modeling (FDM) is one of the most common polymer additive processes, it will be utilized for this study to allow for a wider applicability of results to current

industrial applications. In FDM, polymeric filament is fed by a tractor wheel arrangement into a heated extruder head which deposits the material by tracing a sliced layer of a CAD model [1]. During printing, the extruder head typically moves along an XY plane to trace a layer, followed by a change in the Z direction by dropping the bed or raising the head before printing of the subsequent layer. One of the main reasons for the common use of FDM is the wide material customization offerings due to the ability to fine tune a variety of build parameters. These include but are not limited to layer thickness, layer orientation, raster pattern, raster angle, raster width, raster air gap, bed temperature, extrusion temperature, extrusion speed, nozzle shape and diameter, support pattern, contour width, contour air gap, and number of contours [1].

One of the main polymeric materials of interest for AM is polylactic acid (PLA) as it is both biodegradable and biocompatible. These properties allow it to be used for biomedical components such as bone replacement tissue scaffolds that benefit from intricate customizable patterns [1]. Serra et al. recently were able to create high-resolution PLA-based additively manufactured tissue scaffolds [3]. The improvement of the mechanical properties of these biomedical components could allow for both improved durability and improved performance of the parts. A promising route for improving the mechanical properties of PLA lies in carbon-based reinforcement. Kuan et al. demonstrated that the strength of PLA could be greatly increased with small amounts of multi-walled carbon nanotubes (MWCNT) dispersed in the polymer matrix [4]. Similarly, Pinto et al. showed that the strength and modulus of PLA could be improved with the addition of graphene [5]. PLA is also hydrophilic and must be dried prior to use otherwise flow instabilities will occur upon heating. The particular PLA resin used in this project was the amorphous Natureworks 4060D. 4060D is traditionally used for thin film

applications, however the excellent rheological properties of this grade makes it optimal for AM applications.

Mechanical properties can also be increased through adjustment of the FDM processing parameters such as build speed, build direction in relation to the part orientation, layer thickness, and fill pattern. Halil et al. investigated chopped carbon fiber reinforcement of a similar FDM feedstock, acrylonitrile-butadiene-styrene (ABS), and discovered that while mechanical properties increased with increased fiber loadings, void content within the bead correspondingly increased due to poor interfacial adhesion [6]. Rezayat et al. modeled the relationship between the build parameter structure and the mechanical properties in FDM of ABS, and found that adjusting the air gap in between rasters from negative to positive resulted in a change in the load transfer mechanism from the raster to the contour of the part, implying that statistically relevant tensile results can only be obtained if the build parameters are carefully selected [7]. Ahn further investigated the effect of varying process parameters on the anisotropy of the material properties in FDM, and emphasized that for max tensile loads, the load direction should align with the reinforcement orientation [8]. Torres et al. tested torsional mechanical properties of PLA in FDM and concluded that near-bulk PLA properties could be obtained through specific parameter optimization, however it was also found that while post-process heat treatments slightly increased strength, ductility decreased dramatically [9].

The goal of this project will be to fabricate and test PLA additive feedstock reinforced separately with MWCNT and graphene at 0.5, 0.2 and 0.1 wt% loadings. The mechanical properties of ASTM standard tensile and impact specimens printed with the enhanced feedstocks will be compared to that of specimens printed with un-reinforced PLA. Additionally, the effect of varied reinforcement loadings on the thermal properties of the feedstocks will be investigated

with Differential Scanning Calorimetry (DSC). Morphology, adhesion, and failure analysis studies will be performed using Scanning Electron Microscopy (SEM).

2 Methods

NatureWorks LLC (Minnetonka, MN) 4060D PLA chopped resin was provided by the Carbon and Composites group at Oak Ridge National Laboratory for this project. Graphene was purchased from Celtic LLC (Knoxville, TN) and multiwall carbon nanotubes were purchased from SES Research (Houston, TX). Sample fabrication and testing took place at the University of Tennessee, Knoxville. PLA was heated at 80°C overnight to dry the pellets in a Novatec dessicator. Two masterbatches of PLA composites were produced via dry mixing of 400g PLA and 600g PLA with 1 wt% MWCNT and 1 wt% graphene respectively. The mixtures were extruded at 200°C from a Haake twin screw extruder at a screw speed of 23 rotations per minute for MWCNT composite and 25 rotations per minute for the graphene composite, and both filaments were fed directly into a water bath. The Haake screw was used for its high shear rate leading to effective mixing of the carbon. The master batches were dried overnight and pelletized in a laboratory mill for later use.

Both a Filabot EX2 single screw extruder and Filabot filament winder were provided by the University of Tennessee Department of Materials Science and Engineering for this project. The Filabot extruder was utilized in order to fabricate the AM filament for the 3D printers, but the filament winder proved to be difficult to use properly and was not used. The filament needed to be roughly three millimeters in diameter for proper printing which the maximum available die diameter, so significant process control had to be optimized to maintain a consistent extrusion diameter and avoid filament stretching. The filament production ultimately utilized involved a

small fan pointed at the extrusion nozzle to help the filament cool and, while applying minimal strain, by allowing the filament to slightly drop and then guide it upwards. This decreases the amount of time the filament spends cooling and reduces the strain as well resulting in a fairly consistent filament.

Pure PLA filament was used to print tensile bars designed to Type 1 of ASTM D638 and impact bars designed to the standard in ASTM D256 on a Lulzbot Mini printer. The impact bars were printed with a flat exterior surface and were notched following printing with a specimen notcher. All samples were printed with the same parameters for the purpose of direct comparison.

The masterbatch pellets were mixed with PLA in a single screw extruder to create filaments of graphene and MWCNT composites at 0.1 wt%, 0.2 wt%, and 0.5 wt%. Weight percent loadings were identified based off of results of past research in Dr. Bhat's group.

Maintaining the desired thickness of the filament consistently proved to be very difficult. A very small amount of force could easily apply stress (and therefore strain) to the filament, significantly reducing the diameter of the filament. Several methods were attempted to produce a uniform filament. One was a continuous extrusion to the filament winder, but the filament stuck together and became very thin. Another used a water-bath to quench the filament and maintain the diameter, but the water-bath did not fit directly next to the extruder and the filament still stretched. The manual described a "drop down" method where the filament drops several feet and cools or is dropped into a water bath, but the weight of the filament applied enough stress to deform it significantly. Two fans were obtained to try to increase the airflow around the extruder. One was a basic fan and the other had a water misting option; the latter did not work very well. However, the final method that was determined for use with all of the final filaments is as

follows: the extruded filament, while still hot, can be handled for short periods of time and by running the small fan over the filament and gently leading the filament upwards while applying as little stress as possible, the filament is given sufficient time to cool and maintains the proper diameter and consistency. Furthermore, only small length segments (less than two meters) of the filament are produced at a time to further improve the consistency.

A tensile bar was printed with one of the lower thickness diameter filaments to verify if viable, but it resulted in a much lower quality print with significant voids present. With the proper diameter, the filament prints at a constant deposition rate with an off-white, and reflective appearance. Obtaining a consistent print was the primary reason for utilizing most project time up to this point developing the process for extrusion of three millimeter diameter filament; more consistent prints should result in more consistent results. To further aid in part dimensional stability, a small rectangular void was left in the end pieces of the tensile bars to give the material room to expand and reduce the chance of defects occurring outside the gauge section.

Tensile specimens and impact bars were printed for all of the mixes and tested for direct comparisons. Tensile testing was performed with a SATEC Instron Unidrive tensile testing instrument at a strain rate of 25 mm/min at STP according to ASTM D638. Izod impact properties were tested according to ASTM D256 , with the notches cut post-print from the PLA bars. Scanning Electron Microscopy (SEM) micrographs were taken of fracture surfaces for failure analysis and microstructural evaluation of the specimens, and thermal properties were investigated using differential scanning calorimetry (DSC). DSC sample specimens were removed from post-printed parts, and testing was performed by equilibrating at 30°C, followed by a ramp from 30°C to 200°C at a ramp rate of 5°C per minute.

3 Results & Discussion

Upon beginning to test tensile specimens, it was immediately noticeable that there was significant variation from sample to sample. Within a given composition, some samples would fail quickly, without plastic deformation while others would plastically deform slightly before fracturing. Failure occurred most often as a flat fracture in the middle, but varied in some of the weaker samples. This variation is suspected to be a result of the additive manufacturing process, as there is typically an increase in variation with reference to samples processed through injection molding. Quantitative analysis showed that the graphene composite with 0.2wt% loading had the greatest increase in mechanical properties with a 47% increase in UTS and a 17% increase in Young's Modulus compared to neat PLA. The strongest MWCNT composite occurred at 0.1wt% loading with a respective 41% increase in UTS and 26% increase in Young's Modulus. Additionally, it was seen that there was a minor decrease in ductility in both composites. However it is important to note that both samples has a relatively high variance, and this leads to a low confidence in the increase in strength with compositing. Larger sample sizes would be required to draw conclusions with statistical confidence. Peak loading in both cases occurred at fall smaller loadings than expected by the simply rule of mixtures, and this is partially attributed to the nano-scale of the reinforcement material as reinforcement-reinforcement interactions begin to occur at far lower weight percentages than for micro and macro scale reinforcements.

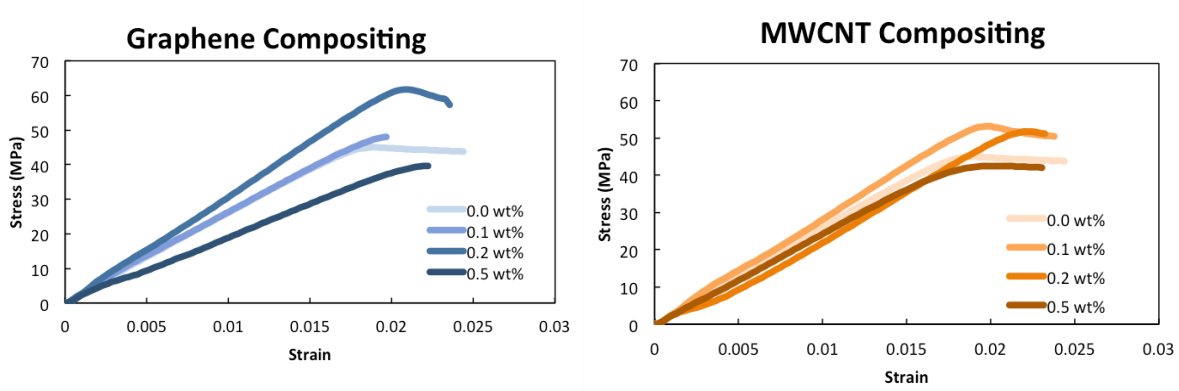

Figure 1. Representative stress-strain curves for all compositions tested

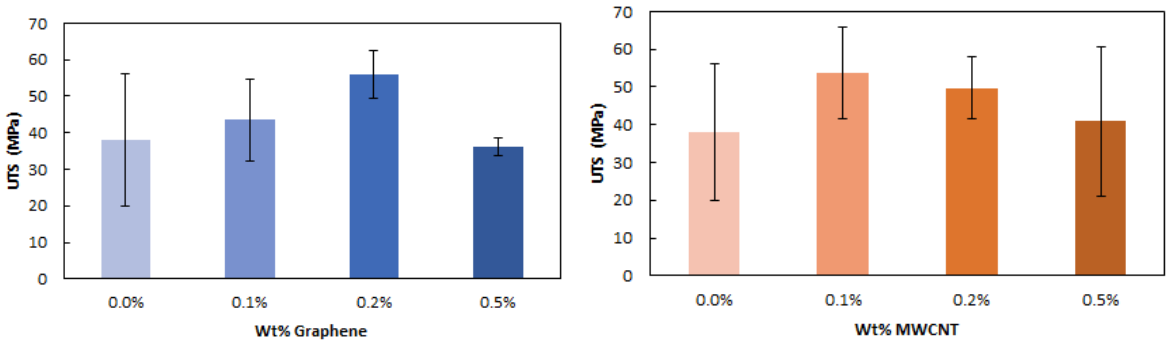

Figure 2. Average UTS of each composition tested. Error bars show one standard deviation of error.

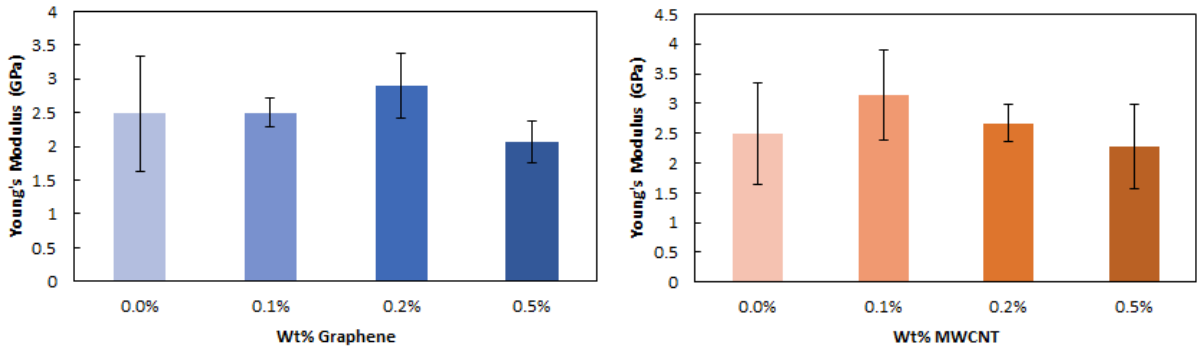

Figure 3. Average Young's Modulus of each composition tested. Error bars show one standard deviation of error.

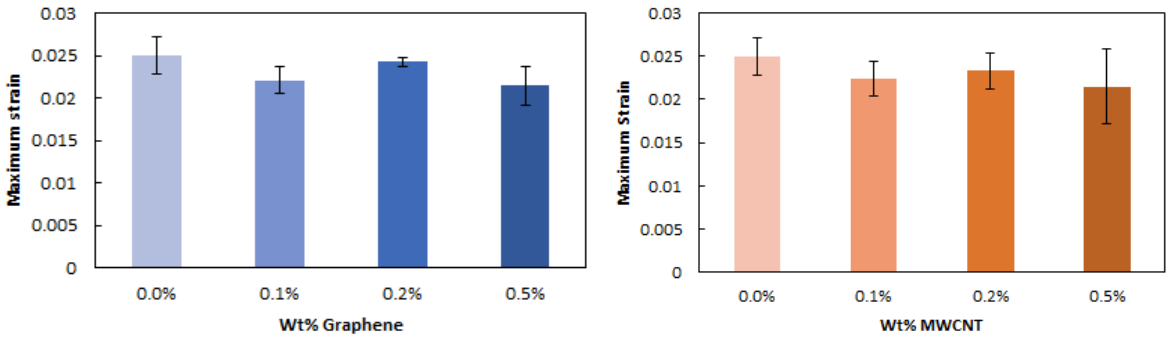

Figure 4. Average maximum strain of each composition tested. Error bars show one standard deviation of error.

One possible source of variation that potentially could have factored into these results is the filament extrusion method, particularly the implementation of the Lulzbot single-screw extruder. Due to a small heating zone and poor geometry, the single-screw extruder could induce some variation in the filament thickness as well as result in mixing inhomogeneities throughout the sample. To have a comparison with commercially viable PLA filament, additional tensile specimens were printed and tested using semi-crystalline PLA filament from Village Plastics. The comparison of this data, with that of our neat in-house produced filament showed that while the elongation data was similar, the Village Plastics PLA had a much higher strength with a smaller variance in this strength. This suggests that our filament production method could induce some additionally decrease in strength and an increase in strength. It is important to mention, however, that semicrystalline PLA tends to be stronger than amorphous PLA, so this likely to be at least part of the contribution to the increase in strength seen in the Village Plastics PLA.

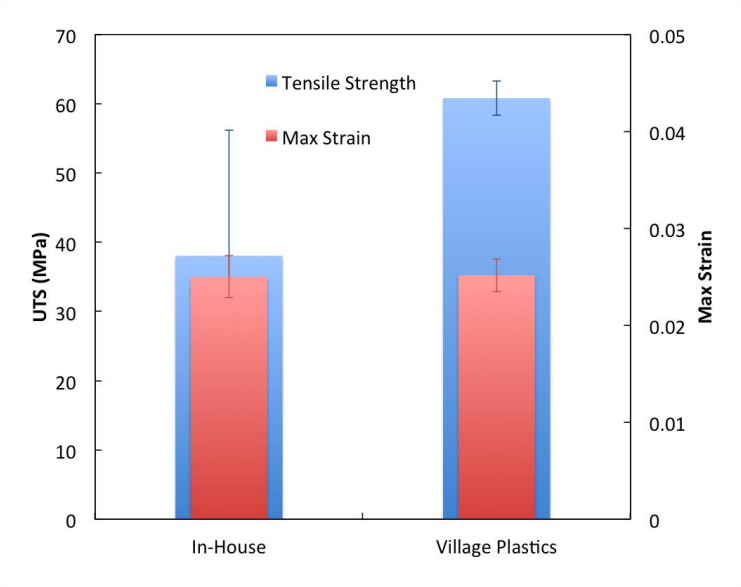

Figure 5. Average tensile strength and max strain of in-house extruded filament compared to Village Plastics filament. Error bars show one standard deviation of error.

SEM analysis, shown partially in Fig. 6, revealed that fracture mechanisms appeared to be similar across all compositions. This suggests that the addition of compositing materials does not induce another fracture mechanism. Additionally, no clumping of either graphene or MWCNTs was found suggesting that the carbon composites were uniformly dispersed within the PLA matrix. The printed filaments can be seen distinctly and that there is significant space between them. Furthermore, there are minor differences between the fracture surfaces, but the overall mechanism remains the same between all samples. All experienced brittle failure where the filaments have been pulled apart as well as showing fracture lines.

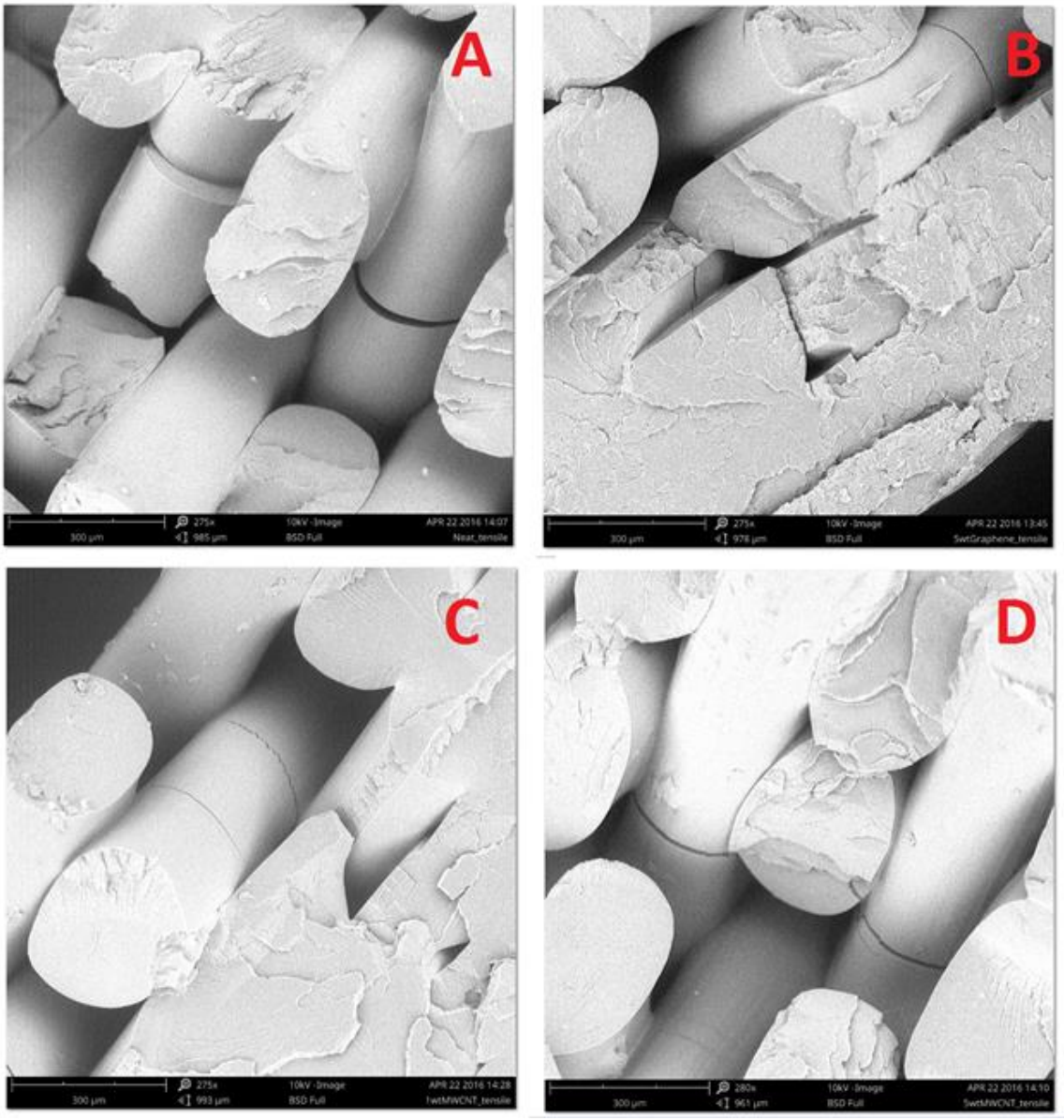

Figure 6. SEM micrographs of various tensile specimens - A: Neat PLA; B: 5wt%Graphene; C:1wt% MWCNT; D: 5wt% MWCNT

DSC results shows no significant change in glass transition temperature with either compositing agent. Additionally, no definitive melt temperature was detected in the neat PLA as it was known to be amorphous. Thus the lack of introduction of a melt temperature signifies that these compositing agents, which are used for catalytics, induced no crystallinity in the PLA. This confirms that increasing loadings of graphene and MWCNT have no significant effect on the

thermal properties of the final parts, which is important to note as if the thermal properties were to vary with reinforcement loadings, the print process window for each sample would have to be individually tailored. This would add an additional level of complexity to industrial standardization of the feedstock production process. However this lack of crystallinity could also indicate an interfacial issue between the composite and matrix.

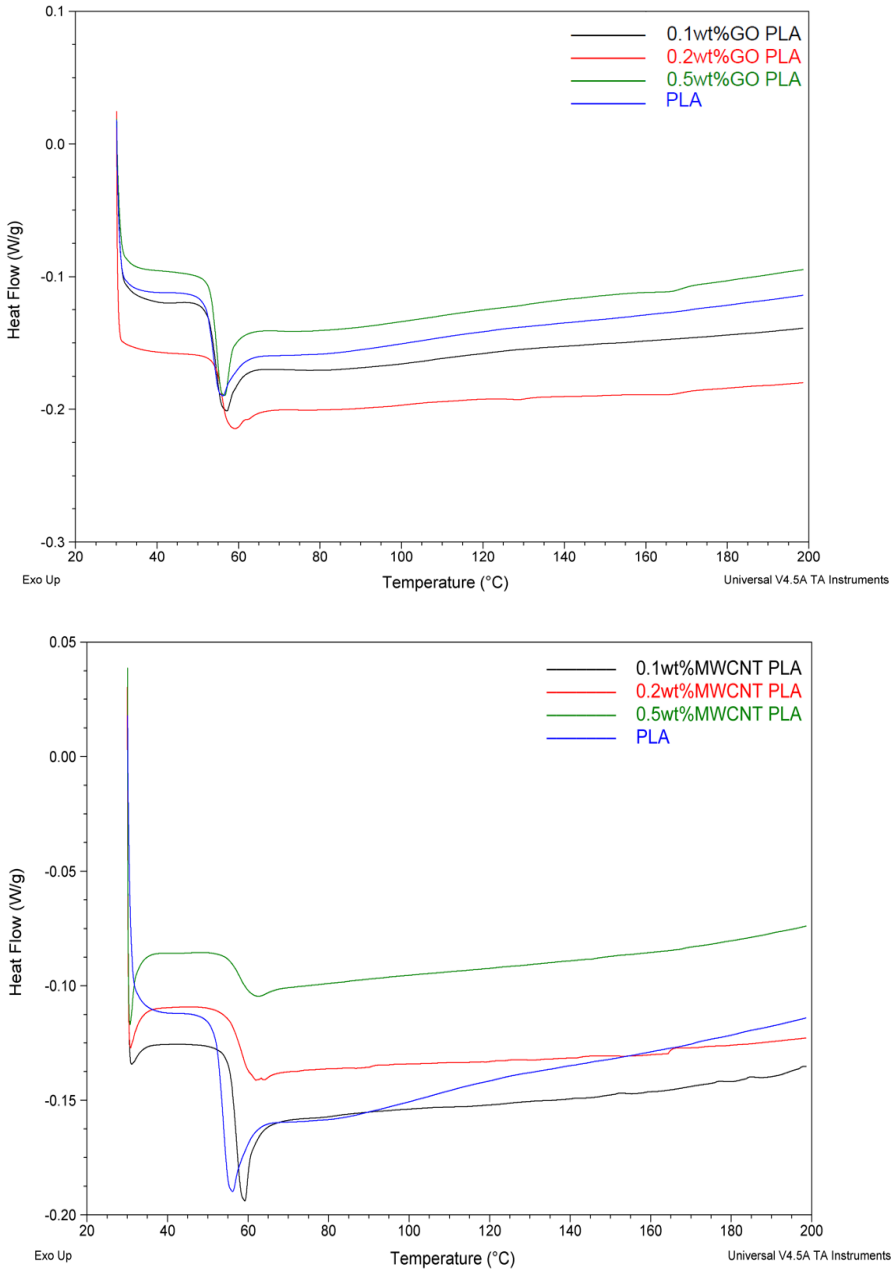

Figure 7. DSC curves comparing increasing loadings of graphene and MWCNT

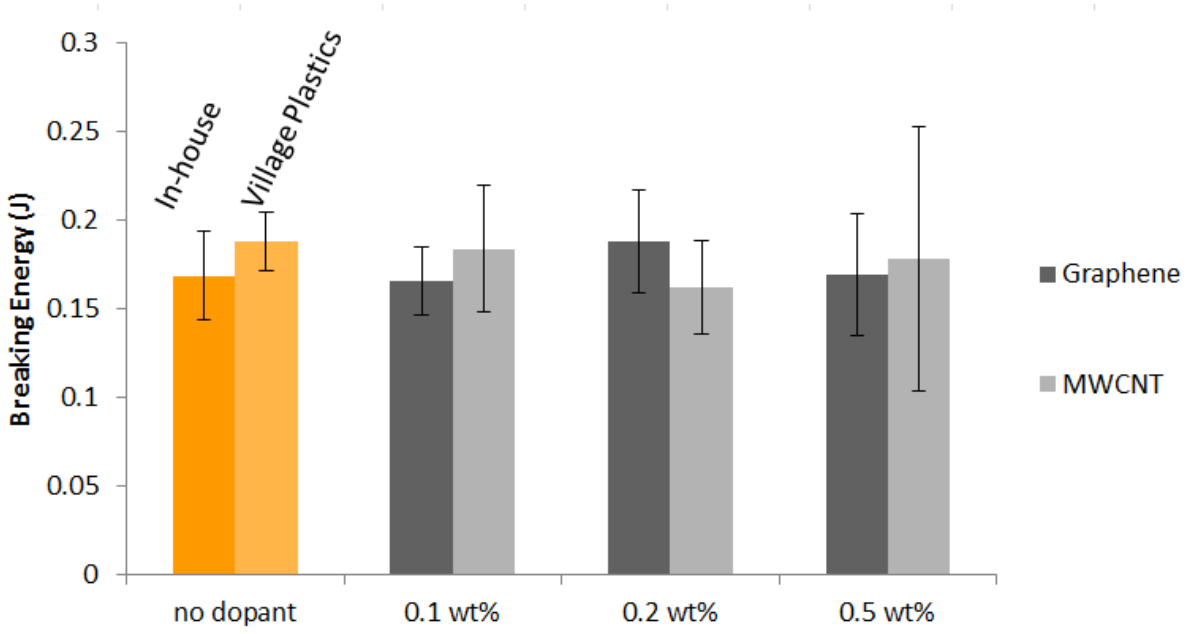

Figure 8. Impact testing results for graphene and carbon nanotube composites and neat in-house and Village Plastics PLA.

The impact data, shown in Fig. 8, followed many of the same patterns previously mentioned with tensile data. With an increase of 11.7% over the in-house produced neat PLA, the 0.2 weight percent graphene had the best overall impact performance, better than even the semicrystalline Village Plastics PLA. The next best composited impact performance came from the 0.1 wt% MWCNT with a 9.2% increase in breaking energy. The increase in breaking energy between in-house extruded PLA and Village Plastics PLA can again largely be explained by the amorphous versus semicrystalline nature, respectively, of the plastics. It must also be noted that the data variation, as seen in the 1σ error bars in Fig. 8, is significant with respect to the data.

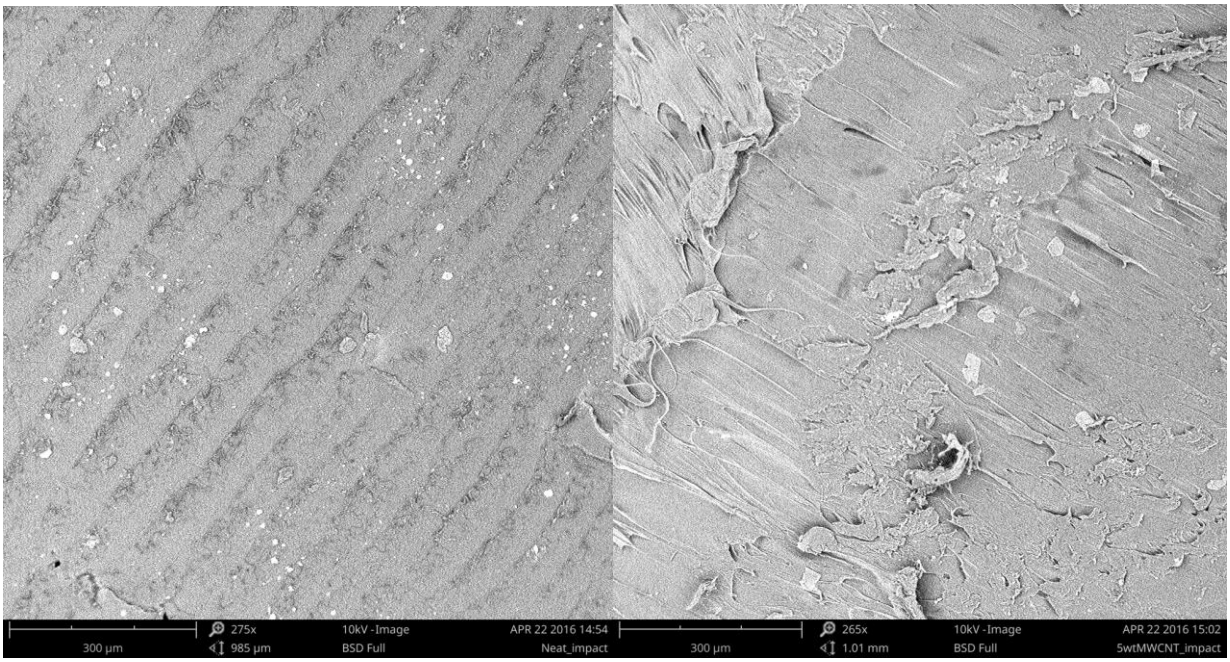

Figure 9. Fracture surface of a neat printed PLA bar (left) and 5 weight percent carbon nanotube printed bar (right).

The fracture surfaces both show that the print layers were sheared together leading to the diagonal lines in both SEM images. Of greater import is the lack of increase in bright spots on the surface of the composited surface over the neat sample, indicating a lack of inclusions, or clustering of the nanoparticles, present in the sample. This trend was seen throughout the other fracture surfaces of graphene and carbon nanotube samples. Lack of clumping is important die as it indicates good mixing of the PLA and shows that strength was not lost due to that failure mode.

4 Conclusions

In the scope of this project, the goal was met. We were able to produce filament with the given materials and test accordingly. Furthermore, minor improvements to the mechanical properties were observed for both graphene and MWCNT, with peak performance seen at 0.2 and 0.1 wt% respectively. The SEM images did not show observable clumping of either the MWCNTs or graphene and showed consistent fracture mechanics which is good from a consistency standpoint. DSC testing showed no change of thermal properties, including a lack of a defined melt temperature which shows that crystallinity was not produced during the extrusion process.

In order to make more concrete conclusions, a decrease of statistical noise is necessary. Larger sample sizes and a more uniform filament production method could decrease the variation in samples produced, and lead to results with greater statistical confidence. Additionally, if continuous filament could be reliably produced, multiple prints could be done at a time rather than having to make single filaments. This would drastically decrease the printing time and allow for it to be run overnight, giving many more testable samples.

Verifying the actual weight percentage of the graphene or MWCNTs throughout each sample is not feasible, and those produced were likely not consistent. In order to have a very even distribution, one would need to create the weight percent batches one by one in the Haake twin screw. This wasn't done in the interest of time, but would likely have a significant impact.

Overall, compositing with either graphene or MWCNT appears to be a promising route to producing strong filaments for the use in additive manufacturing. Additionally, tests that can be performed on these composites that could reveal new areas of applicability could include

characterization of conductivity, dimensional stability, and residual stress of the additive manufactured components.

5 References

[1] I. Gibson, D. Rosen, B. Stucker, *Additive Manufacturing Technologies: 3D Printing, Rapid Prototyping, and Direct Digital Manufacturing*. 2e. 2015

[2] J. R. Fried, *Polymer Science & Technology*. 3e. 2014

[3] T. Serra, J.A. Planell, M. Navarro. “High-resolution PLA-based composite scaffolds via 3-D printing technology.” *Acta Biomaterialia* 9.3 (2013): 5521-5530.

[4] C. Kuan, H. Kuan, C. M. Ma, C. H. Chen. “Mechanical and electrical properties of multi-wall carbon nanotube/poly(lactic acid) composites.” *Journal of Physics and Chemistry of Solids* 69.5-6 (2008): 1395-1398.

[5] A. M. Pinto, J. Cabral, D. A. P. Tanaka, A. M. Mendes, F. D. Magalhaes. “Effect of incorporation of graphene oxide and graphene nanoplatelets on mechanical and gas permeability properties of poly(lactic acid) films.” *Polymer International* 62.33 (2012): 33-40.

[6] H. L. Tekinalp, V. Kunc, G. M. Velez-Garcia, C. E. Duty, L. J. Love, A. K. Naskar, C. A. Blue, and S. Ozcan. “Highly Oriented Carbon Fiber–polymer Composites via Additive Manufacturing." *Composites Science and Technology* 105 (2014): 144-150.

[7] H. Rezayat, W. Zhou, D. Penumadu, and S. S. Babu. "Structure–mechanical Property Relationship in Fused Deposition Modelling." *Materials Science and Technology* 31.8 (2015): 895-903.

[8] S. H. Ahn, M. Montero, D. Odell, S. Roundy, and P. Wright. "Anisotropic Material Properties of Fused Deposition Modeling ABS." *Rapid Prototyping* 8.4 (2002): 248-257.

[9] J. Torres, J. Cotelo, J. Karl, and A. P. Gordon. "Mechanical Property Optimization of FDM PLA in Shear with Multiple Objectives." *JOM* 67.6 (2015): 1183-1193.